Global Temperature Patterns in Past Centuries: An Interactive Presentation

Michael E. Mann,[*,&] Ed Gille,[+] Raymond S. Bradley,[#] Malcolm K. Hughes,[@] Jonathan Overpeck,[+] Frank T. Keimig,[#] and Wendy Gross[+]

* Department of Environmental Sciences, University of Virginia, Charlottesville, Virginia
+ NOAA Paleoclimatology Program, Boulder, Colorado
# Department of Geosciences, University of Massachusetts, Amherst, Massachusetts
@ Laboratory of Tree-Ring Research, The University of Arizona, Tucson, Arizona

Received 11 May 1999; accepted 31 May 2000. (in final form 15 June 2000)

ABSTRACT: The recent availability of global networks of annual or seasonal resolution proxy data, combined with the few long instrumental and historical climate records available during the past few centuries, make it possible now to reconstruct annual and seasonal spatial patterns of temperature variation, as well as hemispheric, global-mean, and regional temperature trends, several centuries back in time.

Reconstructions of large-scale global or hemispheric trends during centuries past can place the instrumental assessments of climate during the twentieth century in a longer-term perspective and provide more robust evidence regarding the roles of potential climate forcings over time. The reconstructed

[&] Corresponding author address: Prof. Michael E. Mann, Department of Environmental Sciences, Clark Hall, University of Virginia, Charlottesville, VA 22903.
E-mail address: mann@virginia.edu

spatial patterns lead to important inferences regarding ENSO-scale variability, the spatial influences of climatic forcings, and the regional patterns that underlie large-scale climate variations. Here proxy-based annual global temperature pattern reconstructions described recently by Mann et al. are expanded upon. For the first time seasonally resolved versions of the proxy-reconstructed surface temperature patterns are presented, and the seasonal differences between key climate indices and patterns of variations are diagnosed. The reader is enabled to interactively examine spatial as well as temporal details (and their uncertainties) of yearly temperatures back in time for both annual-mean and seasonal windows. Annual and seasonal time histories of reconstructed Northern Hemisphere, Southern Hemisphere, and global-mean temperature are made available, as are time histories of the Niño-3 index describing El Niño–related variations, time histories for particular regions of interest such as North America and Europe, and time series for temperature variations in different (e.g., tropical and extratropical) latitude bands. Time histories for specific grid points are available along with their estimated uncertainties. Time histories for the different eigenvectors [i.e., the reconstructed principal components (RPCs)] are also available, along with the raw instrumental series, which underlie the temperature pattern reconstructions. For both the annual-mean and seasonally resolved temperature reconstructions, the reader can directly compare reconstructed patterns for different years, as well as the raw and reconstructed patterns during calibration and verification intervals, and view animated year-by-year sequences of reconstructed global temperature patterns. The statistical relationships between climate forcings and temperature variations are also analyzed in more detail, taking into account potential lagged responses to climate forcings in empirical attribution analyses.

KEYWORDS: Global change; Solar variability; Paleoclimatology; Climate and interannual variability; El Niño

1. Introduction

In order to gauge just how unusual climate trends during the twentieth century truly are, and what the likely causative agents influencing these trends may be, we must rely on indirect lines of evidence to provide a broader context of past climate changes. For assessing some of the broad long-term trends, the history of mountain glacier fluctuations (Grove and Switsur, 1994) and geothermal, borehole-based estimates of past ground temperature (Pollack et al., 1998) can provide important information on climate changes during past centuries. For assessing a year-by-year or even decade-by-decade chronology of such climate changes, however, we must rely upon high-resolution ‘‘proxy’’ climate indicators—natural archives that record seasonal or annual climate conditions such as ice cores, tree-ring measurements, laminated sediments, and corals—combined with the scant available historical documentary or instrumental evidence available in prior centuries.

Increasingly, studies based on the assimilation and analysis of such global ‘‘multiproxy’’ networks of high-resolution proxy climate data have proven useful for assessing global or hemispheric patterns of climate in past centuries (e.g.,

Bradley and Jones, 1993; Hughes and Diaz, 1994; Lean et al., 1995; Mann et al., 1995; Jones et al., 1998; Crowley and Lowery, 2000) and reconstructing climate trends in particularly sensitive, high-latitude regions (Overpeck et al., 1997; Briffa et al., 1998). Such studies have been spurred by hopes to better constrain the influences of natural and anthropogenic factors on long-term climate variability and change (Lean et al., 1995; Overpeck et al., 1997; Mann et al., 1998), to estimate climate sensitivity to external radiative forcing (Crowley and Kim, 1999; Waple et al., 2000), and to validate the behavior of climate models on multidecadal and longer timescales (Barnett et al., 1996; Jones et al., 1998; Delworth and Mann, 2000).

Most recently, global multiproxy climate data have been used to calibrate global-scale patterns of temperature on a yearly basis, several centuries in time by Mann et al. (Mann et al., 1998). The reliability of these reconstructions was demonstrated by cross-validation with independent data, and uncertainties back in time were assessed. These reconstructions have since been extended to estimate Northern Hemisphere (NH) temperature variations over the past millennium (Mann et al., 1999), to examine ENSO-scale patterns of climate variability during past centuries (Mann et al., 2000), to compare observed patterns of variability in the Atlantic with natural coupled ocean–atmosphere modes evident in long climate model integrations (Delworth and Mann, 2000), and to assess the relationship between global patterns of climate variation and particular regional patterns such as the North Atlantic oscillation (NAO) (Mann, 2000; Cullen et al., 2000) Here we further expand on the results of the Mann et al. (Mann et al., 1998) study. We make available for the first time seasonally resolved versions global surface temperature patterns based on the data and methods described in that study. These reconstructions, as well as the original annual-mean reconstructions of Mann et al. (Mann et al., 1998), are made available in a ‘‘user friendly’’ interactive forum, allowing readers to select the particular spatial regions and time periods of particular interest. We also examine in greater detail than before issues related to the sensitivity of the climate reconstructions to varying networks of proxy data, the regional and latitudinal details of past climate variability, and the detection of natural and anthropogenic influences on past temperature changes. We encourage readers to investigate the details of the temperature reconstructions themselves through an interactive graphical user interface. It is our intent here to provide information about past climate changes for consumption by a broad, multidisciplinary readership. Details regarding regional variations, verification or ‘‘cross-validation,’’ and uncertainties inherent in the reconstructions are stressed, so as to encourage a prudent interpretation of proxy-based estimates of past climate changes.

2. Review of data and methods

Details about the data and methods used are provided by Mann et al. (Mann et al., 1998; Mann et al., 1999). The most important aspects of the data and methods used in that study are summarized here for the benefit of the reader. In Figure 1 we show the distribution of proxy and long instrumental data that compose the multiproxy network used by Mann et al. (Mann et al., 1998).

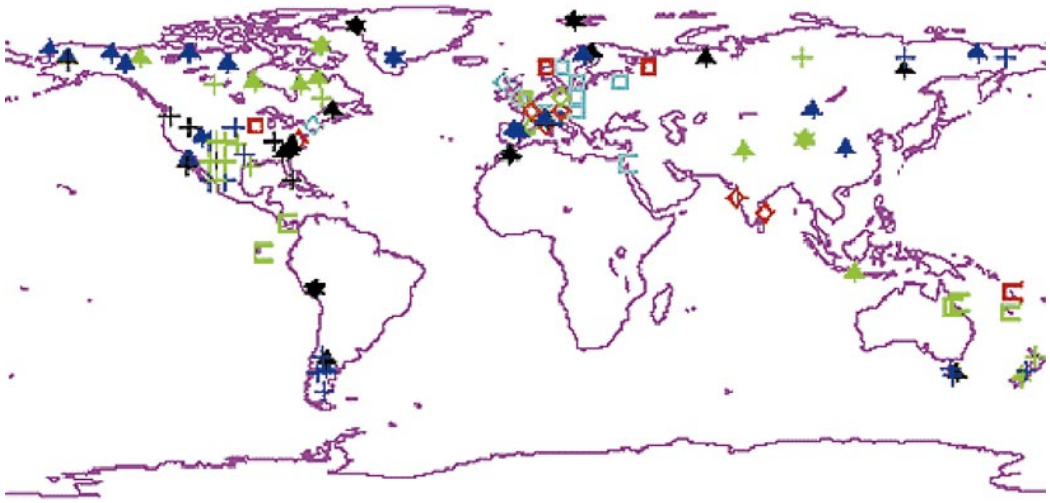

Figure 1. Distribution of annual resolution proxy indicators used in this study. Dendroclimatic reconstructions are indicated by tree symbols, ice core/ice melt proxies by star symbols, and coral records by C symbols. Long historical records and instrumental "gridpoint" series are shown by squares (temperature), or diamonds (precipitation). Groups of plus (+) symbols indicate principal components of dense tree-ring subnetworks, with the number of such symbols indicating the number of retained principal components. Sites are shown dating back to at least 1820 (red), 1800 (blue-green), 1750 (green), 1600 (blue), and 1400 (black). Certain sites (e.g., the Quelccaya ice core) consist of multiple proxy indicators (e.g., multiple cores, and both oxygen isotope and accumulation measurements). [Reprinted with permission from Mann et al. (Mann et al. 1998).]

These data were calibrated (see details in Mann et al., 1998) by the instrumental surface temperature data (Figure 2) available during the twentieth century, based on a multivariate regression of the proxy data network against the primary eigenvectors of the monthly global instrumental temperature data (Figure 3) to yield a statistical relationship that would allow the projection of temperature patterns on a year-by-year basis, preceding the twentieth century (1902–80) period of widespread instrumental data. The spatial temperature patterns were determined by summing over the reconstructed histories of the retained eigenvectors RPCs. The reader is referred to Mann et al. (Mann et al., 1998) for details regarding the calibration process. In the present study, the entire procedure has been repeated for two distinct half-year seasons: the boreal warm season/austral cold season (Apr–Sep) and the boreal cold season/austral warm season (Oct–Mar). [Note: It is our convention to reference the boreal cold season reconstructions to the year corresponding to Jan–Mar rather than Oct–Dec. This differs by 1 yr from certain other conventions (e.g., the typical convention for referring to winter-mean Southern Oscillation index (SOI) and should be kept in mind in making comparisons with other winter climate indices.] The results of the temperature pattern calibra-

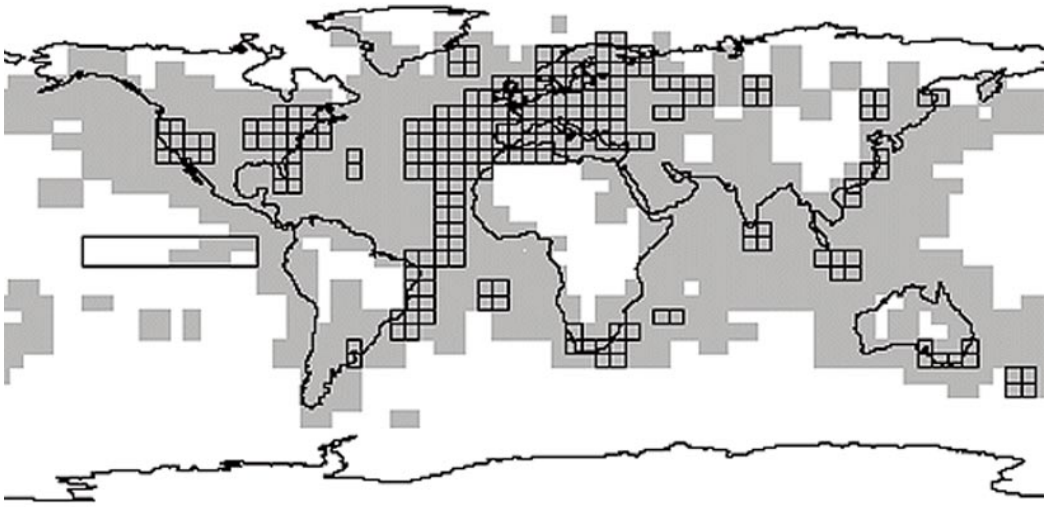

Figure 2. Distribution of the (1082) nearly continuous available monthly land air–sea surface temperature gridpoint data available from 1902 onward indicated by shading. The squares indicate the subset of 219 grid points with nearly continuous records extending back to 1854 that are used for verification. Northern Hemisphere (NH) and global (GLB) mean temperature are estimated as areally weighted (i.e., cosine latitude) averages over the Northern Hemisphere and global domains, respectively. The large rectangle indicates the tropical Pacific SST subdomain discussed in the text. The small rectangle in the eastern tropical Pacific shows the traditional Niño-3 region. These data are described in more detail by Jones (Jones, 1994). [Initial comparisons using an updated version of this dataset (e.g., Jones et al., 1999) showed no significant differences in the large-scale structure of the twentieth century surface temperature dataset, although some specific differences are notable, particularly during the World War II years (e.g., the mid-1940s). Future updates of these reconstructions will employ this latter instrumental surface temperature dataset.] [Reprinted with permission from Mann et al. (Mann et al. 1998).]

tions for both the annual-mean reconstructions of Mann et al. (Mann et al., 1998) and the more recent seasonal (boreal cold and warm half-year) reconstructions are provided for the reader.

The validity of the annual-mean reconstructions was demonstrated based on a series of statistical cross-validation or ‘‘verification’’ experiments. In these experiments, the reconstructions based on the calibration of twentieth century instrumental data were compared against withheld instrumental data, including those available on a large-scale basis during the latter half of the nineteenth century (see Figure 4), and sparser data available in certain regions (e.g., Europe and North America) several centuries back in time. The reader is referred to Mann et al. (Mann et al., 1998) for details of these experiments. We provide here the

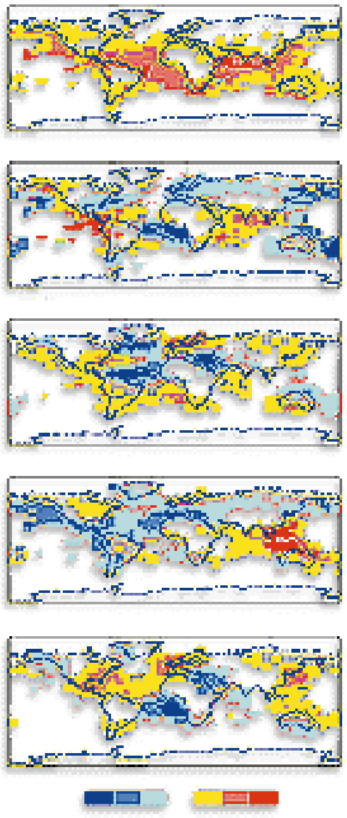

Figure 3. Empirical orthogonal functions (EOFs) for the five leading eigenvectors of the global temperature data from 1902 to1993. [Reprinted with permission from Mann et al. (Mann et al. 1998).]

actual statistical results from the verification experiments for the annual mean, cold season, and warm season. (The results are available online: annual, http://www.ngdc.noaa.gov/paleo/ei/stats-supp-annual.html; cold season, http://www.ngdc.noaa.gov/paleo/ei/stats-supp-cold.html; warm season, http://www.ngdc.noaa.gov/paleo/ei/stats-supp-warm.html.) The reconstructions have been demonstrated to be unbiased back in time, as the uncalibrated variance during the twentieth century calibration period was shown to be consistent with a normal distribution (Figure 5) and with a white noise spectrum. Unbiased self-consistent estimates of the uncertainties in the reconstructions were consequently available based on the residual variance uncalibrated by increasingly sparse multiproxy networks back in time. [This was shown to hold up for reconstructions back to about 1600. For reconstructions farther back in time, Mann et al. (Mann et al., 1999) show that the spectrum of the calibration residuals is somewhat more ''red,'' and more care needs to be taken in estimating the considerably expanded uncertainties farther back in time.]

These various internal consistency checks and verification experiments, to-

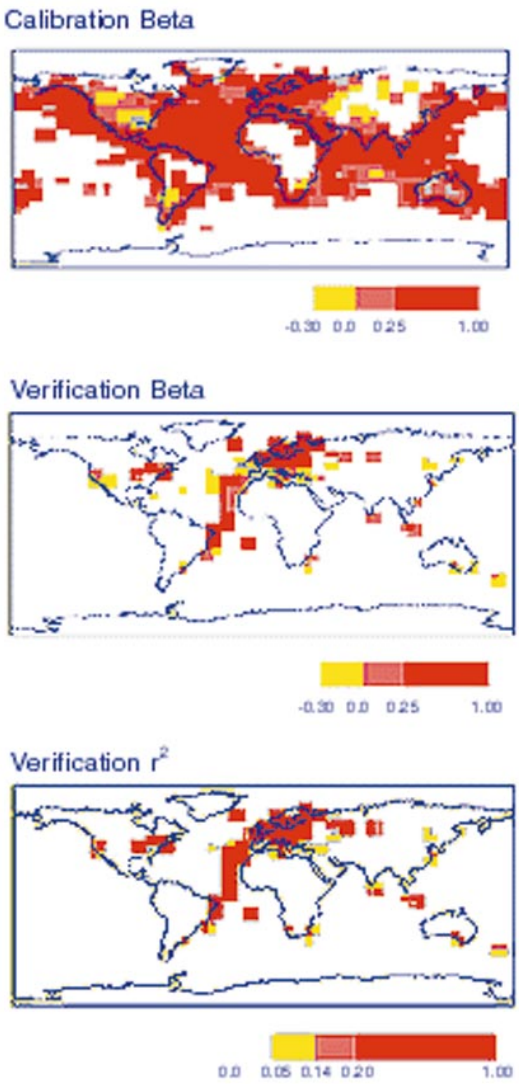

Figure 4. Spatial patterns of (top) calibration beta, (middle) verification beta, and (bottom) *r*-squared statistics for annual-mean reconstructions. The calibration statistics are based on the 1902–80 data, while the verification statistics are based on the sparser 1854–1901 instrumental data (see Figure 2) withheld from calibration. For the beta statistic, values that are insignificant at the 99% level are shown in gray, while negative, but 99% significant values are shown in yellow, and significant positive values are shown in two shades of red. For the *r*-squared statistic, statistically insignificant values (or any grid points with unphysical negative values of correlation) are indicated in gray. The color scale indicates values significant at the 90% (yellow), 99% (light red), and 99.9% (dark red) levels (these significance levels are slightly higher for the calibration statistics that are based on a longer period of time). More details regarding significance level estimation are provided in Mann et al. (Mann et al, 1998). [Reprinted with permission from Mann et al. (Mann et al., 1998).]

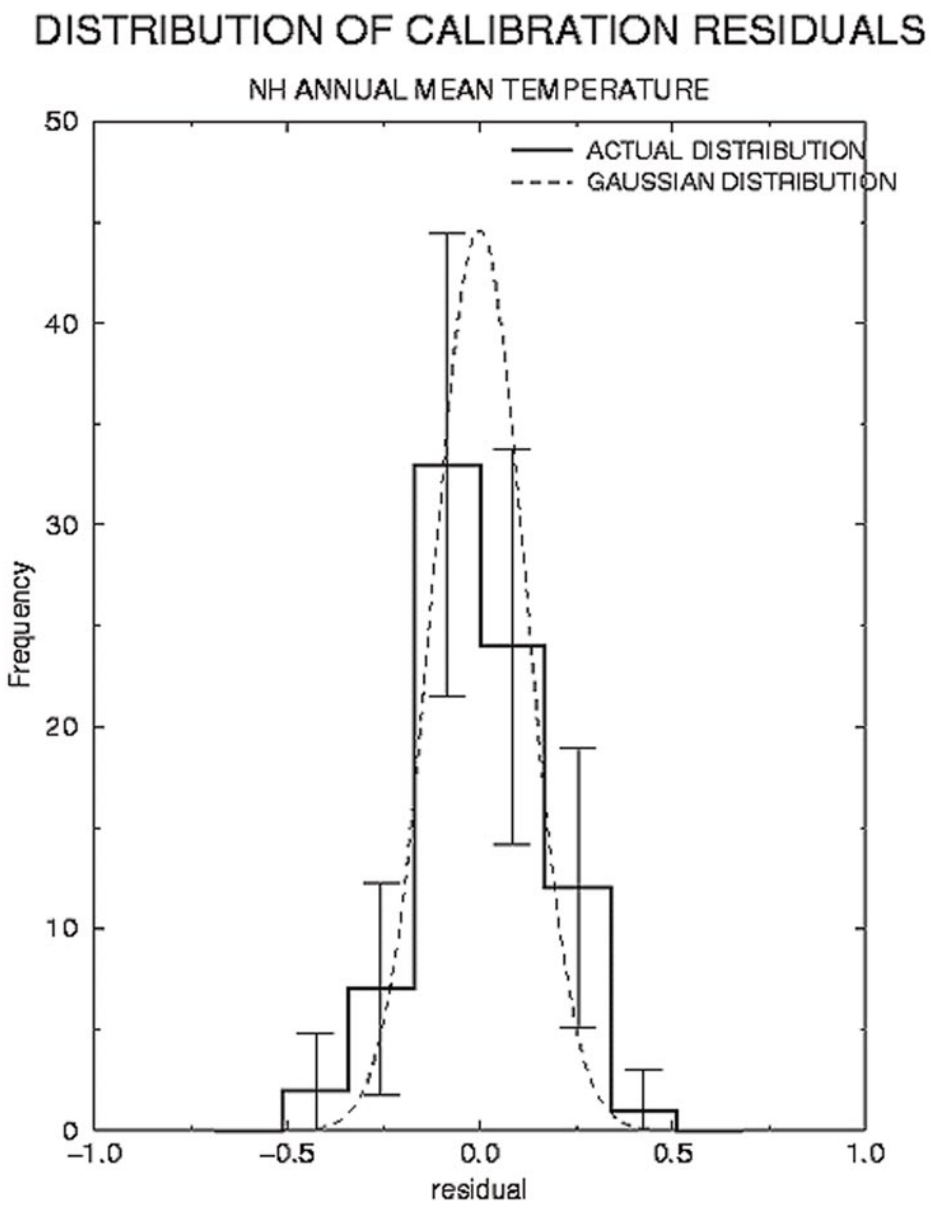

Figure 5. Histogram of calibration residuals for annual-mean NH series. A Gaussian parent distribution is shown for comparison, along with the ±2 standard error bars for the frequencies of each bin. The distributions are consistent with a Gaussian distribution at a high (95%) level of confidence. The distribution of residuals for the Niño-3 index (not shown) is consistent with a Gaussian distribution at a 99% level of confidence.

gether, indicate that skillful and unbiased reconstructions are possible several centuries back in time, both for the annual mean and independent cold and warm seasons. However, the reader will note that a considerably smaller fraction of the instrumental variance is calibrated in the seasonal reconstructions (particularly the warm season) than in the annual-mean reconstructions. We attribute this to the constructive mutual seasonal information in the diverse network of proxy data used, which allows more effective reconstruction of annual-mean conditions than particular seasonal conditions. The uncertainties are thus considerably greater for the seasonal reconstructions. Moreover, the annual-mean reconstructions are not equivalent to the sum of the cold-season and warm-season reconstructions since the substantially greater uncertainties in the latter add in quadrature, rather than canceling, in a numerical average. For example, the amplitude of the NH series variations in past centuries is similarly underestimated for both warm and cold seasons, and the average of the two is a considerable underestimate of the annual-mean reconstruction. For these reasons, the quantitative details of these latter reconstructions should be interpreted quite cautiously, although the qualitative insights afforded by the seasonally resolved versions of the reconstructions are useful.

Owing to the decreased number of spatial degrees of freedom in the earliest reconstructions (associated with significantly decreased calibrated variance before, e.g., 1730 for annual-mean and cold-season pattern reconstructions, and about 1750 for warm-season pattern reconstructions) regional inferences are most meaningful in the mid–eighteenth century and later, while the largest-scale averages are useful farther back in time. For example, the NH annual-mean temperature series appears to exhibit skill back to at least A.D. 1400 [and has now been extended back to A.D. 1000 by Mann et al. (Mann et al., 1999), albeit with expanded uncertainty estimates]. We have also verified that possible low-frequency bias due to nonclimatic influences on dendroclimatic (tree ring) indicators is not problematic in our temperature reconstructions. (A note on possible nonclimatic tree-ring trend bias is available online: http://www.ngdc.noaa.gov/paleo/ei/ei_nodendro.html.)

A Niño-3 SST index, describing El Niño–related variability, can be calculated in the eastern tropical Pacific directly from these reconstructions (i.e., by averaging the global reconstructions over the Niño-3 rectangular region defined in Figure 2). The Niño-3 reconstructions are also discussed in more detail in the next section.

3. Temperature reconstructions

In this section, we describe, present, and interpret the annual and seasonal temperature reconstructions, associated uncertainties, and raw data used in calibration and verification.

3.1. Large-scale trends

The reconstructed annual Northern Hemisphere mean temperature series is shown in Figure 6. Based on this reconstruction, Mann et al. (Mann et al., 1998) argued

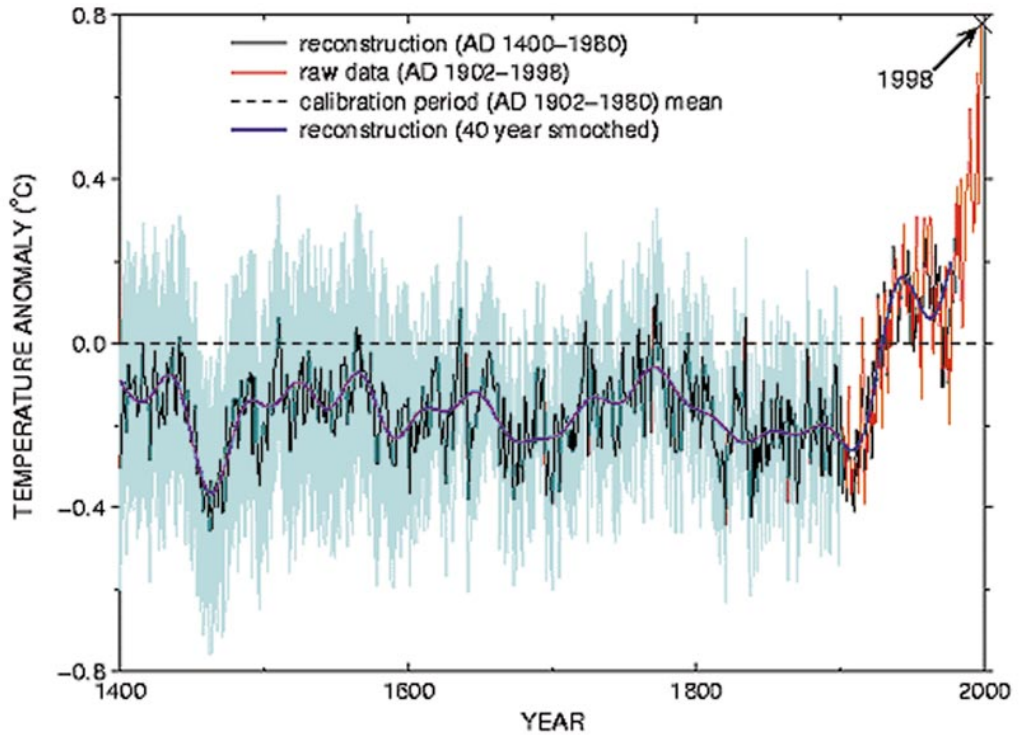

Figure 6. Northern Hemisphere mean temperature reconstruction from A.D. 1400–1980, shown with raw instrumental NH series (red) through 1998. The low-frequency trend (timescales longer than 40 yr emphasized) is shown by the thick curve. The blue-shaded region indicates the two standard error uncertainty limits in the reconstruction (see Mann et al., 1998 for details). Additional data are available online at ftp://ftp.ngdc.noaa.gov/paleo/paleocean/by_contributor/mann1998/mannnhem.dat.

that the warmth of the 1990s (three years in particular: 1990, 1995, 1997) was unprecedented in at least the past 600 years, taking into account the self-consistently estimated uncertainties in the reconstruction back to A.D. 1400. Based on the most recent extensions of this reconstruction (Mann et al., 1999), it furthermore now appears that 1998 was likely to have been the warmest year of at least the past millennium. (Millennium reconstructions are available online: http://www.ngdc.noaa.gov/paleo/ei/ei_millenm.html.)

The raw NH annual-mean series used for calibration (based on the full sampling available during the 1902–80 calibration period; see Figure 2) and verification (based on the sparser sampling available during the 1854–1901 verification interval; see also Figure 2) are also shown (Figure 7) along with the reconstructed NH series constructed from the corresponding spatial samplings (this is for the sake of comparison with the available instrumental record back in time; the NH series reconstruction discussed elsewhere is based on the full spatial sampling of

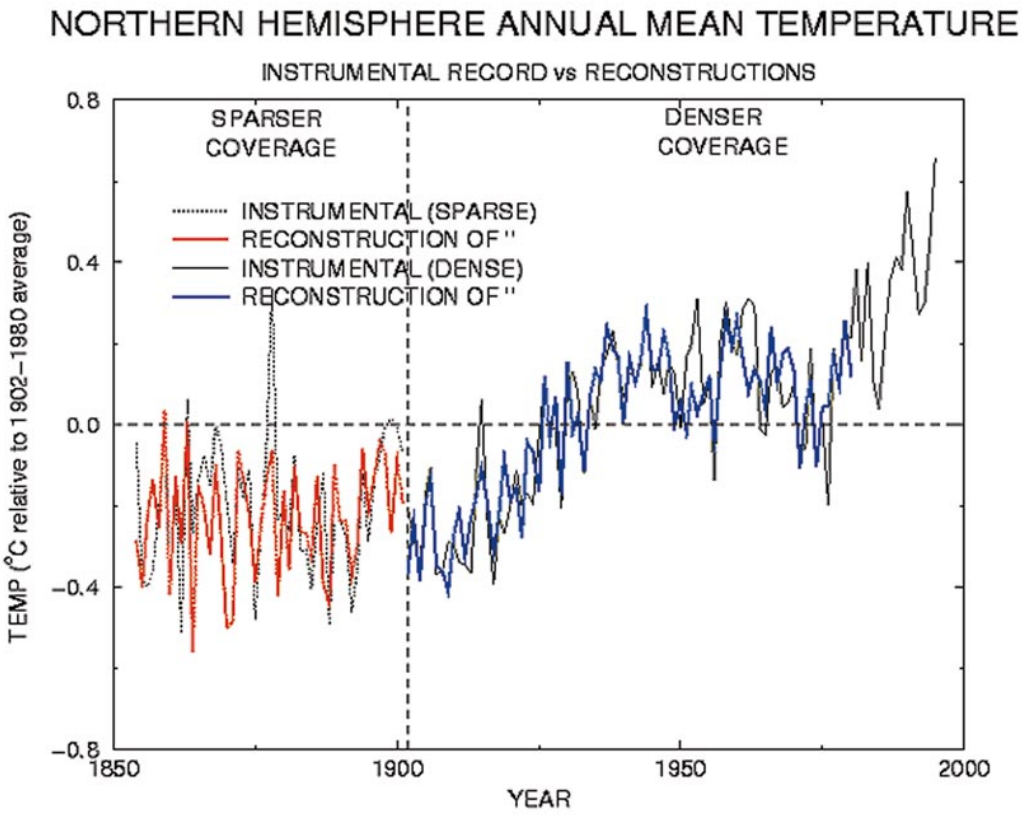

Figure 7. Reconstructed NH mean temperature series vs raw instrumental NH series from 1854 to 1980. For the purposes of a meaningful comparison, the NH spatial means have in this case been diagnosed in both the raw data and reconstructions from the sparse gridpoint coverage of the verification period from 1854 to 1901 (ftp://ftp.ngdc.noaa.gov/paleo/paleocean/by_contributor/mann1998/nhem-sparse.dat), and the dense coverage of the calibration period from 1902 to 1980 (ftp://ftp.ngdc.noaa.gov/paleo/paleocean/by_contributor/mann1998/nhem-dense.dat).

the calibration period, which is implicit in the pattern reconstructions back in time). The good overall correspondence between the reconstructed NH series in both calibration and independent verification intervals visually confirms the quantitative indications of statistical skill discussed earlier.

We focus on the NH mean temperature series because it is the most reliable hemispheric estimate given the available spatial sampling in the surface temperature fields (Figure 2). Nonetheless, Southern Hemisphere (SH) and global (GLB) mean temperatures can be diagnosed from the appropriate areally weighted averages of the available spatial sampling in the pattern reconstructions. Taking into account the limitations in these latter estimates (the SH sampling is almost entirely

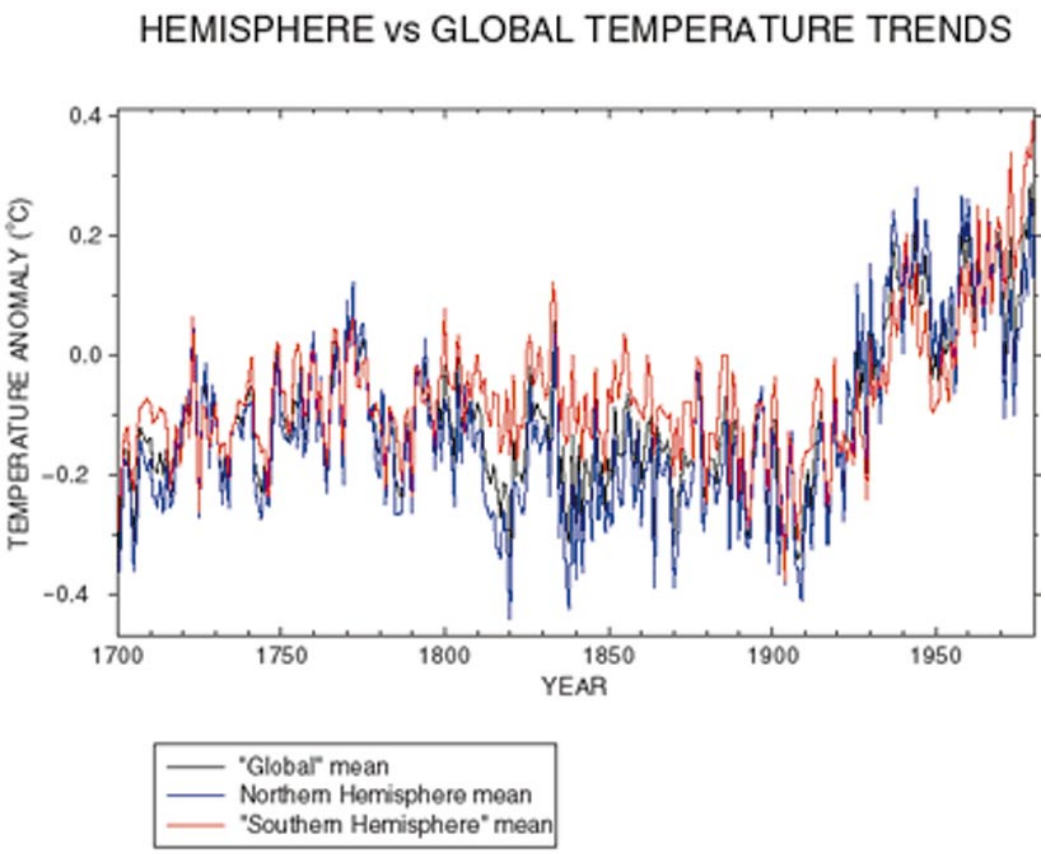

Figure 8. Comparison of reconstucted annual-mean temperature trends for Southern Hemisphere, Northern Hemisphere, and global mean, diagnosed from the available spatial sampling (Figure 1). Additional data are available online at http://www.ngdc.noaa.gov/paleo/ei/ei_reconsa.html.

tropical and subtropical, and the GLB estimate is necessarily dominated by the coverage in the Northern Hemisphere half of the domain), some interesting conclusions can be drawn. While the two hemispheres (NH and SH series) show similar temperature trends during the past few centuries (Figure 8), the coldness of the nineteenth century appears to be somewhat more pronounced for the Northern Hemisphere. The GLB series, dominated by the Northern Hemisphere half of the domain, shows similar character to the NH series. Only through assembling a greater distribution of both instrumental and proxy data in the Southern Hemisphere will it be possible to calculate truly meaningful estimates of Southern Hemisphere and global temperature variations during past centuries.

It is also instructive to examine the trends in different latitude bands. Overpeck et al. (Overpeck et al., 1997) suggested that post-1850 warming was more dramatic at high northern latitudes relative to lower latitudes due to larger positive feedbacks at high latitudes. The annual-mean temperature trends at high latitudes

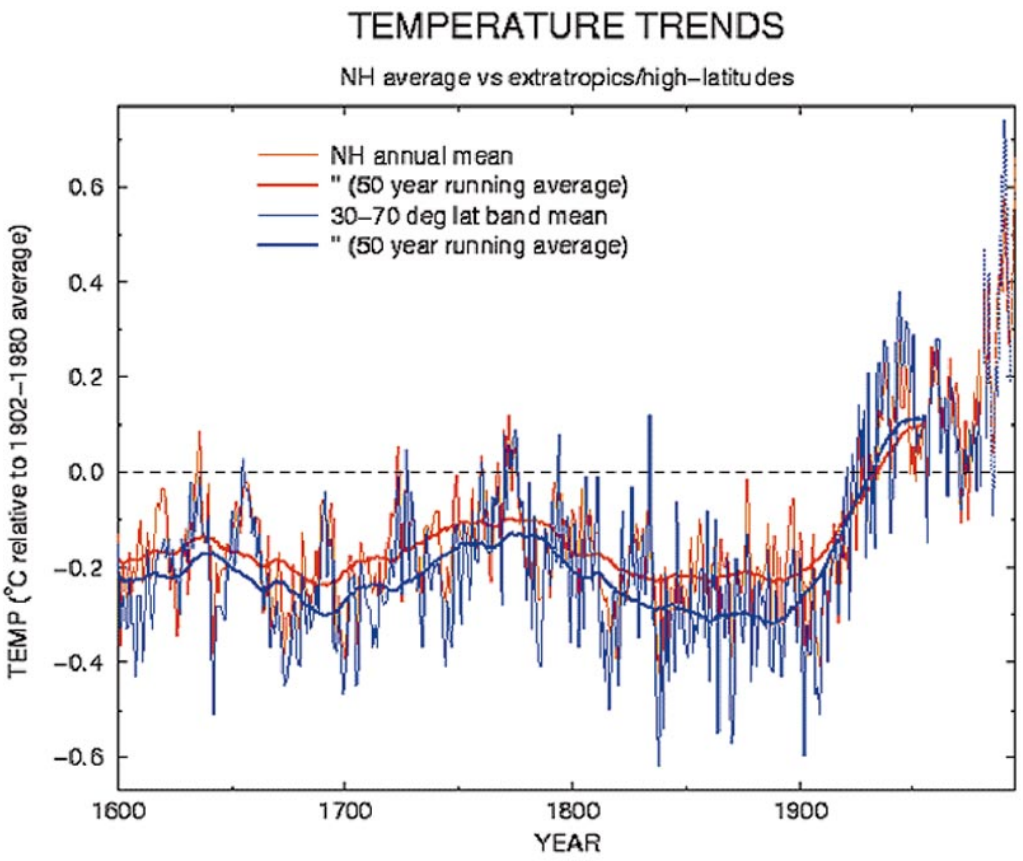

Figure 9. Reconstructed annual-mean NH mean temperature series based on full latitudinal coverage (red) vs the average reconstructed series for the extratropical latitude 30°–70°N band (blue). Additional data are available online: http://www.ngdc.noaa.gov/paleo/ei/ei_reconsa.html.

are seen (Figure 9) to be greater than the hemispheric trends themselves. In contrast, the tropical (30°S–30°N) band shows less change than the entire Northern Hemisphere series.

It is also instructive to compare hemispheric trends with other more regional temperature trends. In Figure 10, we show the reconstructed NH series along with an areal-mean reconstruction over the North American region, during the past few centuries. It is clear that the nineteenth century was especially cold in North America (approximately 0.6°C colder than the entire NH mean), and the subsequent warming trend of the twentieth century accordingly more dramatic (i.e., approximate 1.2° vs 0.6°C). The fluctuations are significantly greater on almost all timescales for the North American series, which is simply a consequence of the spatial sampling statistics of a smaller region. It is thus clear that one would be remiss in drawing conclusions regarding hemispheric-scale temperature changes from such highly variable regional temperature estimates, underscoring the

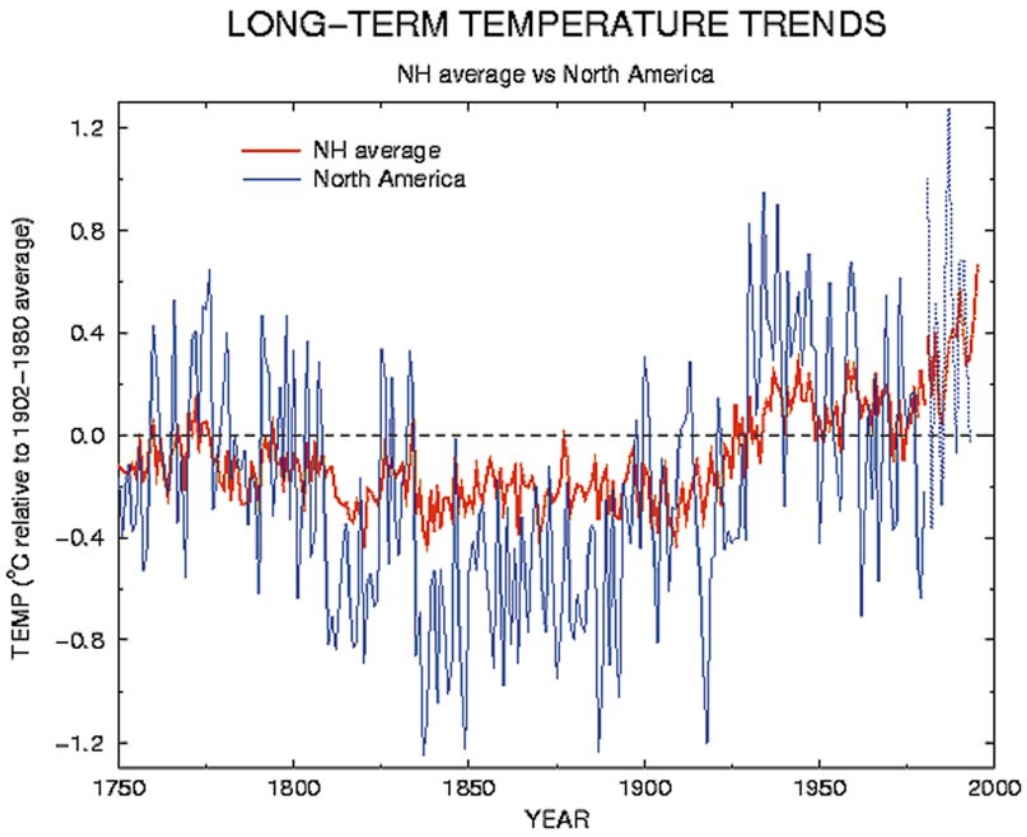

Figure 10. Comparison of reconstructed NH (red) and North American (blue) regional temperature variations during past centuries.

importance of drawing inferences from the largest-scale mean trends in which regional ‘‘noise’’ is dampened and certain types of signals (e.g., the influence of climate forcings, discussed later) are more clearly detected. Seasonal distinctions are also clearly important. For example, it is clear that interannual fluctuations in European cold-season temperatures are considerably greater than those during the warm season (Figure 11). This observation is consistent with the impact of the large year-to-year variability in the predominantly cold-season NAO phenomenon (see, e.g., Luterbacher et al., 1999; Mann, 2000; Cullen et al., 2000). The impact of the NAO and detailed regional inferences are discussed in detail in the subsequent section.

We also provide the time histories of the first five RPC series (along with their raw counterparts from 1902 to 1993; see Figure 12). Note that the RPCs are available for different lengths back in time owing to the decreasing spatial degrees of freedom resolved by the multiproxy network back in time (see Mann et al., 1998 for a discussion).

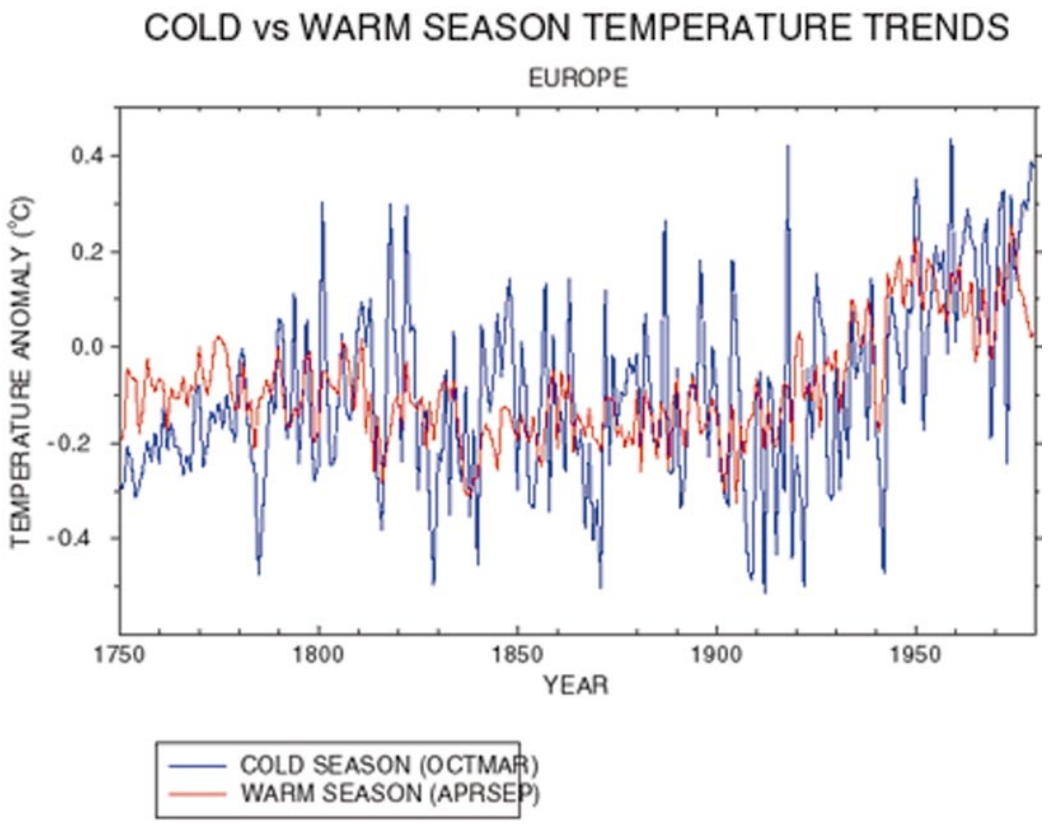

Figure 11. Comparison of European temperature trends back to 1750 for cold and warm half-year seasonal windows.

3.2. Spatial patterns

Yearly global temperature maps for annual mean, boreal cold season, and warm season are available below for the reconstructed temperature fields (1730–1980), the raw temperature data (1902–93) used for calibration, and the sparse raw ''verification'' temperature data (1854–1901) used for cross-validation. Also available are the ''EOF filtered'' instrumental data from 1902 to 1993. In the latter case, only that data variance during the calibration period described by the actual eigenvectors used to calibrate the multiproxy network (see section 2) is retained. These filtered versions of the raw data are thus in some sense a more appropriate standard for comparison to the multiproxy-reconstructed patterns than the raw data themselves.

Raw data and reconstructed patterns can be compared side by side where available. These maps are ''clickable'' so that time series for particular regions (with uncertainties, in the case of reconstructions) can be obtained. Movie 1 shows the temperature fields.

To investigate the spatial patterns and time histories of the global temperature

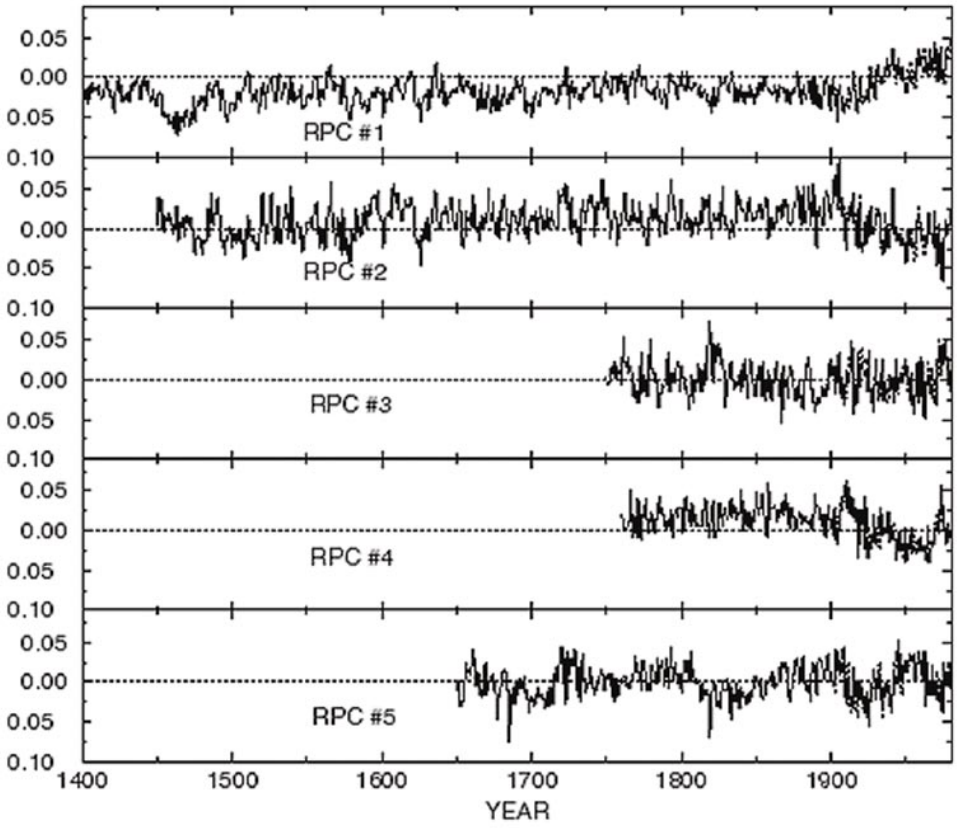

Figure 12. RPC series for the first five eigenvectors (see Figure 3) back in time, along with their twentieth century instrumental counterparts. Annual-mean and seasonal RPC data can be found online at the bottom of the following Web page: http://www.ngdc.noaa.gov/paleo/ei/ei_reconsa.html.

reconstructions, readers can begin by visiting the following site online: http://www.ngdc.noaa.gov/cgi-bin/paleo/mannplot2.pl, where maps such as the one for 1730 shown below can be viewed.

In part due to the especially strong El Niño of 1997–98, there has been renewed interest in past variations in the El Niño phenomenon, and the context in which they place prominent recent (1997–98 and 1982–83) events. Two excellent examples of past very strong El Niños in the reconstructions are those evident in the temperature patterns for 1791 and 1878 (Figure 13). Independent corroboration of these events is provided by the historical chronology of Quinn and Neal (Quinn and Neal, 1992; see also Mann et al., 1998). The reader may note that an improvement upon this historical El Niño chronology has recently

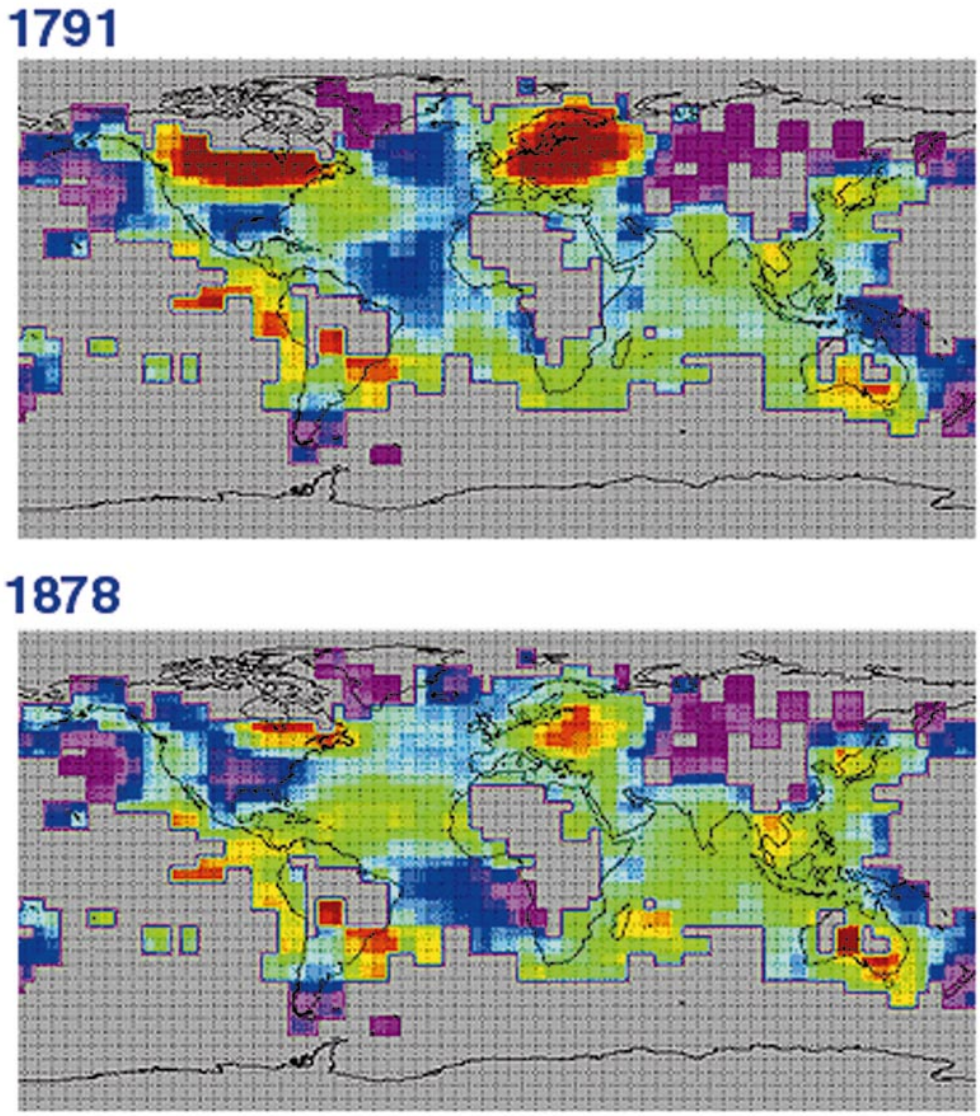

Figure 13. Global temperature pattern reconstructions for two historically documented very strong El Niño events during (top) 1791 and (bottom) 1878.

been provided by Ortlieb (Ortlieb, 2000), with conclusions that sometimes differ from those of Quinn and Neal (Quinn and Neal, 1992). We note, however, that, to the extent that the Quinn and Neal chronology used here is imperfect, it will provide a very conservative corroboration of our own chronology, as mismatch may be due to uncertainties in the chronology as well as in our reconstruction. Both events shown exhibit the classic eastern tropical Pacific warming and horseshoe pattern of warming and cooling in the North Pacific. The details of ENSO-

related patterns of variation in the annual-mean temperature reconstructions are discussed by Mann et al. (Mann et al., 2000).

The reconstructed annual-mean Niño-3 index provides an estimate of El Niño–related temperature variability in our reconstructions. Based on this index, the 1997–98 and 1982–83 events appeared (see the discussion in Mann et al., 2000) to be among the strongest events back to at least A.D. 1650. However, it could not be concluded with much certainty at that time that they are stronger than any other events during that period, owing to the appreciable uncertainties in the reconstructions for the tropical Pacific region and the suboptimal calendar-mean basis for that reconstruction.

However, as is evident in the statistics, the cold-season Niño-3 index calibrates/cross-validates a considerably larger share of the instrumental data variance than the annual-mean series (about 50% in calibration and verification back to 1780, and about 40% back to 1650). This is not surprising because a boreal cold-season window is a more appropriate basis for defining the ENSO phenomenon than a calendar mean. Our winter Niño-3 reconstruction exhibits a highly significant correlation with largely independent reconstruction of the winter (Dec–Jan–Feb) SOI of Stahle et al. (Stahle et al., 1998). The two reconstructions are correlated at $r = 0.63$ over the full period of overlap (1705–1976) and $r = 0.60$ during the precalibration interval (1705–1901). This is nearly as high as the observed correlation ($r = 0.7$) between the instrumental SOI and Niño-3 series during the twentieth century. The similarity of these two reconstructions, as well as the significant correspondence with the historically based El Niño chronology of Quinn and Neal (Quinn and Neal, 1992) discussed earlier (see cold-season calibration/verification statistics available online: http://www.ngdc.noaa.gov/paleo/ei/ei_calverif.html), suggests considerable reliability in the ENSO-related features of our surface temperature reconstructions. Using this improved, seasonal reconstruction of Niño-3 (Figure 14) we find added evidence that the two recent events, 1982–83 and 1997–98, stand out as somewhat anomalous in the long-term record. There is evidence that certain events (such as the 1877–78 El Niño) may be more underestimated in their amplitude in our reconstruction than would be expected from random calibration uncertainties. This is difficult to determine, as the instrumental surface temperature record is quite sparse during that period of time. Moreover (see Mann et al., 2000), the winter SOI, used as a substitute for the Niño-3 index, shows quite similar behavior to our reconstruction at that time. Only further work with both the instrumental record and proxy climate records in ENSO-sensitive regions will further elucidate this issue. (Annual-mean Niño-3 indices are available online at http://www.ngdc.noaa.gov/paleo/ei/ei_Niño-3ann.html and Niño-3 cold-season data are available at http://www.ngdc.noaa.gov/paleo/ei/ei_data/Niñocold-recon.dat.)

As commented upon earlier, there are important distinctions between regional and hemispheric trends, with regional trends exhibiting considerably greater variability and heterogeneity. Cold and warm periods in different parts of the globe, for example, are not in general synchronous. Even during the ‘‘Little Ice Age’’ (Bradley and Jones, 1993) not all areas were uniformly cold; geographical and temporal variations were apparent, as highlighted by an examination of the re-

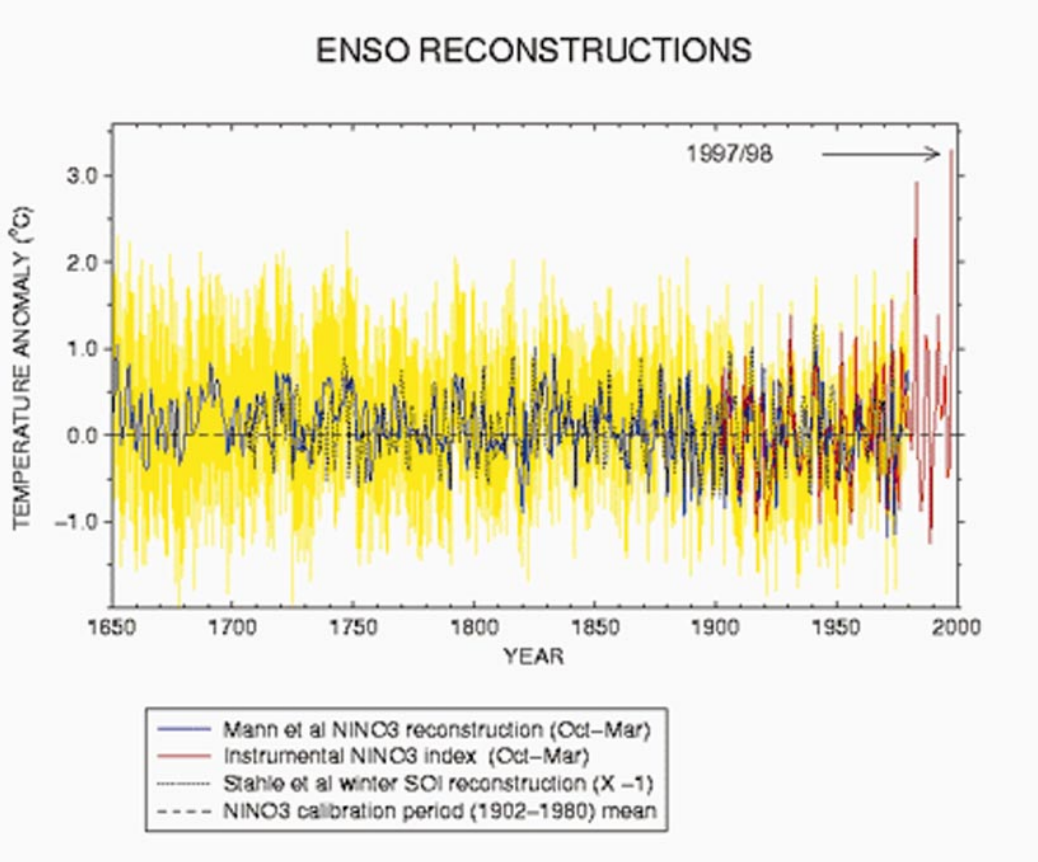

Figure 14. Reconstructed boreal cold-season Niño-3 index back to 1650. Shown for comparison is a partially independent (dendroclimatic rather than multiproxy) winter (DFJ) reconstruction of the SOI (Stahle et al., 1998). Yellow-shaded region indicates the 95% confidence bounds for the Niño-3 reconstruction.

constructions presented here. The ‘‘Medieval Warm Period’’ or ‘‘Medieval Optimum’’ (Hughes and Diaz, 1994) is even more enigmatic.

It is sometimes erroneously argued that the globe was as warm or even warmer than present during the early part of the millennium (e.g., A.D. 1000–1200) based on historical or anecdotal considerations (e.g., the early colonization of Greenland, unusually bountiful agricultural yields and wine harvests in Europe early in the millennium, etc.). Mann et al. (Mann et al., 2000) use a careful statistical analysis to show that the sparse regional information available earlier than A.D. 1400, while allowing for verifiable hemispheric temperature reconstructions back to about A.D. 1000, is associated with self-consistent estimates of uncertainties that are greatly expanded beyond those during more recent centuries.

These limitations notwithstanding, the best evidence, based on the extension of hemispheric climate reconstructions back a full millennium, is that late twen-

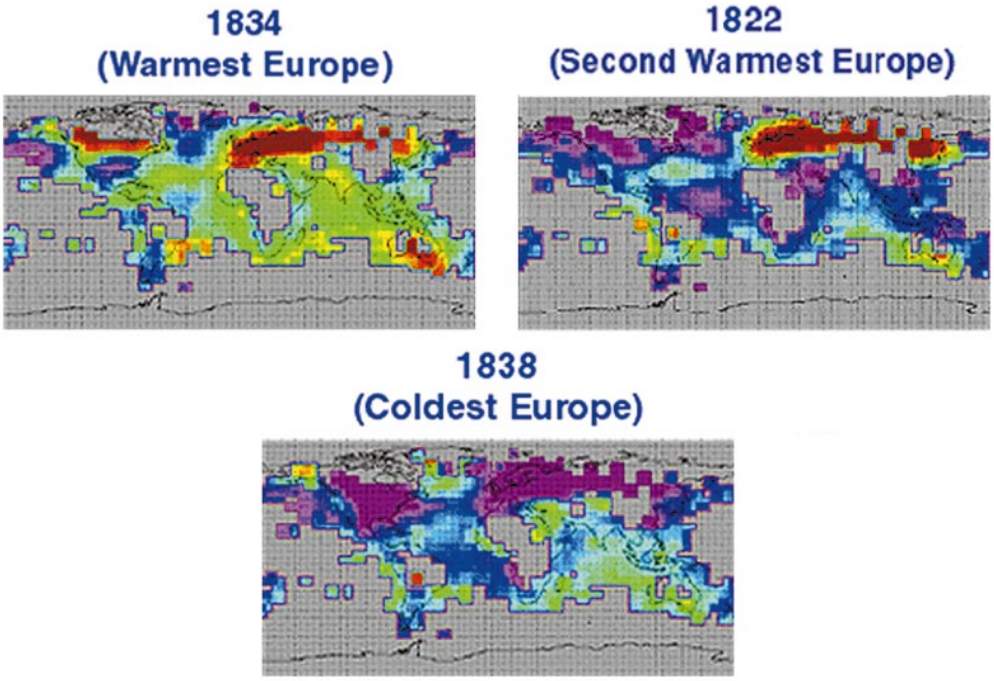

Figure 15. Global annual-mean temperature pattern reconstructions for three years associated with unusually warm or cold anomalies in the European sector during (top, left) 1834, (top, right)1822, and (left) 1838.

tieth century conditions are probably warmer than those that prevailed at any time this millennium, though conditions during the eleventh through fourteenth centuries appear warmer than those that prevailed during the fifteenth through nineteenth centuries in general. This conclusion is supported by independent estimates based on composites of modest numbers of Northern Hemisphere proxy records (Jones et al., 1998; Crowley and Lowery, 2000). The nineteenth century was particularly cold for *both* Europe and North America (the reader is referred to the regionally averaged temperature series for North America and Europe here). This period comes closest to being a truly ''global'' cold period (see Mann et al., 1999) although, as noted earlier, even in this case the cooling is not nearly as evident in the Southern Hemisphere.

To illustrate some of the problems inherent in estimating hemispheric mean temperature from limited regional information, consider (Figure 15) the warmest (1834), second warmest (1822), and coldest (1838) years in Europe prior to the twentieth century, based on the Mann et al. (Mann et al., 1998) temperature pattern reconstructions.

While 1834 was the warmest year in Europe, it was colder than typical conditions (by twentieth century standards) over large parts of the Northern Hemisphere. This is especially true for 1822, the second warmest year in Europe, but

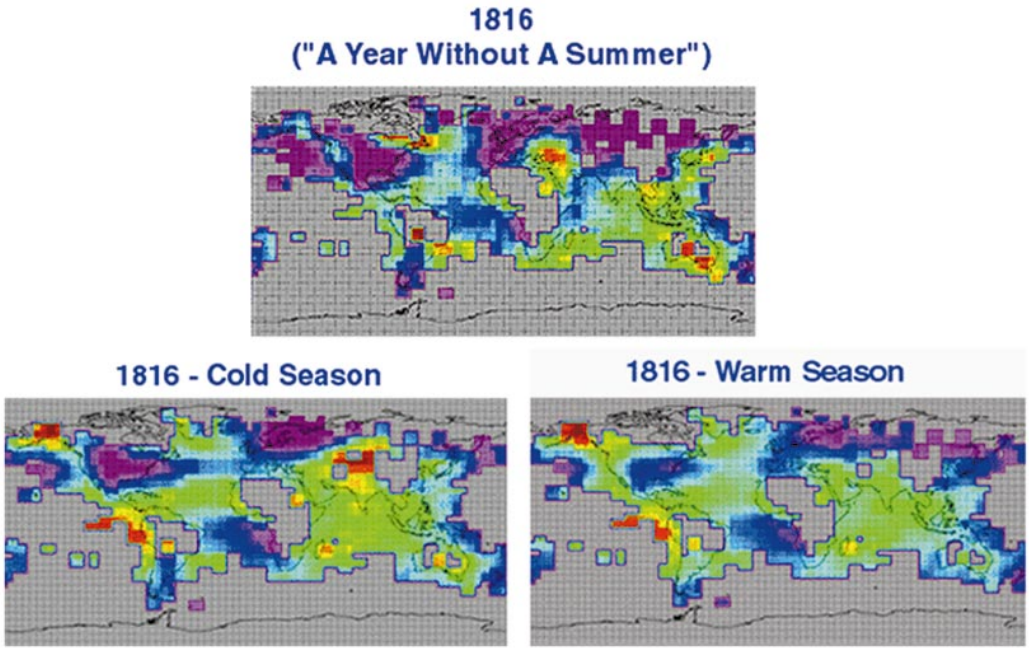

Figure 16. Annual-mean global temperature pattern reconstructions for the so-called year without a summer—1816.

a cold year over most of the Northern Hemisphere. In contrast, the coldest year in Europe (1838) was indeed one of the coldest over much of the Northern Hemisphere (see discussion below), but in fact, temperatures were nonetheless warm, relative to typical twentieth century conditions, over significant portions of Greenland and Alaska. The coldest years in Europe might, by analogy with this example, have been quite unusually mild in Greenland, and a favorable opportunity for its colonization. It becomes readily evident from such examples (let alone, more careful statistical diagnostics) that inferences into hemispheric or global-scale temperature variations based on limited regional (e.g., European) information are perilous. In fact, the considerable low-frequency ‘‘noise’’ in the Atlantic and neighboring regions, due in large part to modes of ocean circulation variability (see, e.g., Delworth and Mann, 2000), and the substantial overprint of the North Atlantic oscillation on climate variations in this region during past centuries (see, e.g., Cullen et al., 2000; Mann, 2000) particularly obscures hemispheric trends in this region. There is modeling evidence, in fact, that suggests that medieval warmth was restricted to regions influenced by the North Atlantic (Overpeck, 1998). Statistically speaking, estimates of European temperature variability provide a very poor indication of large-scale temperature trends in past centuries, and should be strictly avoided for hemispheric, let alone global scale, climate inferences.

Note that 1816 (the so-called year without a summer; Figure 16), in addition to appearing to have indeed been an especially cold summer (see Briffa et al.,

1998) and a cold year for the NH temperature as a whole (though not anomalous relative to other years during that very cold decade), was an anomalously cold year only in Europe and parts of North America. In fact, conditions in the Middle and Near East were warmer than normal by twentieth century standards.

A number of other years (1870, 1864, 1838, 1820, 1700, 1642, and many years during the 1450s and 1460s) appear to have been *substantially* colder than 1816 for the hemisphere as a whole in the temperature reconstructions presented here. Our notions of this year as a particularly cold one may thus arise in large part from the fact that the coldness was most pronounced in those regions—Europe and North America—that figure most prominently in the western anecdotal and historical framework. The regional overprints of warming (e.g., in the Middle East) and extreme cold (e.g., Europe) that are superimposed on generally cold hemispheric conditions, in regions neighboring the North Atlantic, may be attributed to the NAO [see Luterbacher et al. (Luterbacher et al., 1999), Cullen et al.(Cullen et al., 2000), and Mann (Mann, 2000) for a discussion of inferences into past NAO-related climate variability]. We believe that both the cold hemispheric conditions, and a strong NAO-like atmospheric circulation anomaly, were due to the explosive Tambora eruption in Indonesia during spring of 1815 (see Mann et al., 1998). Seasonally specific reconstructions of 1816 for the cold (Oct–Mar) and warm (Apr–Sep) half-years (see Figure 16) indicate that this pattern is clearer and more dominant during the cold season, wherein the quadrapole pattern of warm and cold anomalies in continental regions bordering the North Atlantic is quite distinct. This is as expected, since the NAO is primarily, though not exclusively, a cold-season mode of atmospheric circulation variability. There is some evidence of the persistence of this pattern, albeit more weakly, into the warm season. In particular, distinct cooling in the eastern United States and over much of Europe is clearly expressed during the warm season, consistent with the notion of 1816 having been a year without a summer in those regions. Some of the coldness of the early nineteenth century might also be due to weakened solar irradiance forcing at that time. The possible influences of external climate forcings on hemispheric temperatures are discussed below.

3.3. Influence of climate forcings

The statistical relationship between variations in NH mean temperature and estimates of the histories (see Mann et al., 1998) of solar, greenhouse gas, and volcanic forcings is shown in Figure 17. [For a note about the difference between the plot shown herein and that shown in Mann et al. (Mann et al., 1998), see http://www.ngdc.noaa.gov/paleo/ei/ei_attriold.html.]

While the natural (solar and volcanic) forcings appear to be important factors governing the natural variations of temperatures in past centuries, only human greenhouse gas forcing alone, as noted by Mann et al. (Mann et al., 1998), can statistically explain the unusual warmth of the past few decades. The possible influences of regional industrial aerosol cooling during the latter part of the twentieth century (see Houghton et al., 1995) were not included in our attribution analysis, and this cooling may in fact mask an even stronger greenhouse gas signal during the past few decades.

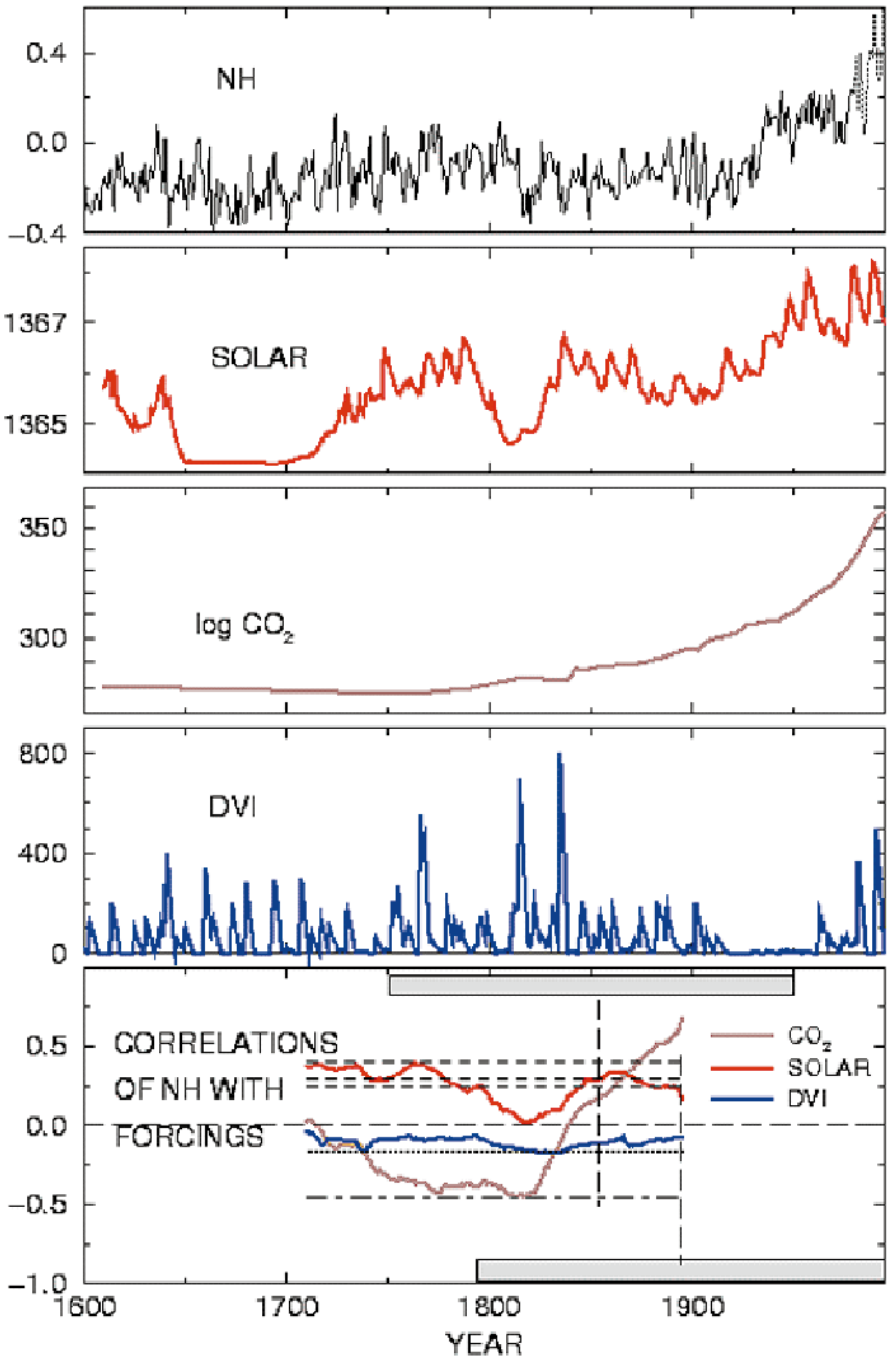

Figure 17. Relationship of annual-mean NH mean temperature reconstruction to estimates of three candidate forcings (see Mann et al., 1998) between 1610 and 1995.

Mann et al. (Mann et al., 1998) noted that the contemporaneous (i.e., zero delay) response to forcings implicit in their statistical attribution analysis may underestimate the true, lagged responses to forcing. Volcanic responses appear to be slightly greater and more consistently significant about 1 yr following the eruption (see Briffa et al., 1998), while the response of the climate to global radiative forcings should be significantly delayed [e.g., 10–20 yr based on most sensitivity estimates; see Houghton et al. (Houghton et al., 1995)] by the thermal inertia of the oceans. In Figure 18 we investigate possible such lagged relationships to forcing. We also examine the sensitivity of the time-dependent attribution approach discussed above to employing a shorter (100 yr) window. A complementary approach to the attribution of forcings involves the use of a climate model forced with estimated histories of greenhouse, volcanic, and solar radiative forcings to estimate the expected large-scale temperature trends in past centuries. Preliminary results of such an experiment (Robertson et al., 1998) show a favorable comparison with our hemispheric temperature reconstructions.

From the above analysis it is clear that when physically reasonable lags are incorporated into the attribution analysis, there is evidence of even greater statis-

←

Figure 17. (continued) (a) Reconstructed NH temperature series from 1610 to 1980, updated with raw data from 1981 to 1995. (b) GHGs represented by atmospheric CO_2 measurements. (c) Reconstructed solar irradiance (see Lean et al., 1995). (d) Weighted volcanic dust veil index (DVI). (e) Evolving multivariate correlation of NH series with the three forcings (a, b, and c).

The time axis denotes the center of a 200-yr moving correlation window. Significance levels are based on the null hypothesis that the surface temperature series is a realization of natural variability represented as represented by a red noise process with the persistence structure of the observed NH series (see Mann et al., 1998 for details). One-sided significance levels for correlations with the different forcing agents are shown, under the assumption that only positive relationships with GHG and CO_2, and negative relationships with DVI, are physically meaningful. These confidence levels are approximately constant over time and are thus represented by their average values over time for simplicity (although the number of degrees of freedom in the CO_2 series is somewhat decreased prior to 1800 when the series is essentially flat, so that the confidence intervals are slightly too liberal in this case). Significance levels for correlations of temperature with CO_2 and solar irradiance are nearly identical, and the 90%, 95%, and 99% (positive) significance levels are shown by the horizontal dashed lines. The 95% (negative) significance level for DVI is shown by a horizontal dotted line. The lower dotted line indicates the 99% significance level for correlation with GHG if a *two-sided* hypothesis test is invoked (this is only added to emphasize that the seemingly spurious negative correlation of NH with GHG apparent during the late eighteenth–early nineteenth century is in fact not statistically significant if the a priori physical requirement of a positive relationship between CO_2 and temperature is not taken into account in hypothesis testing). The gray bars indicate two different 200-yr windows of data in the moving correlation, with the long-dashed vertical lines indicating the center of the corresponding windows.

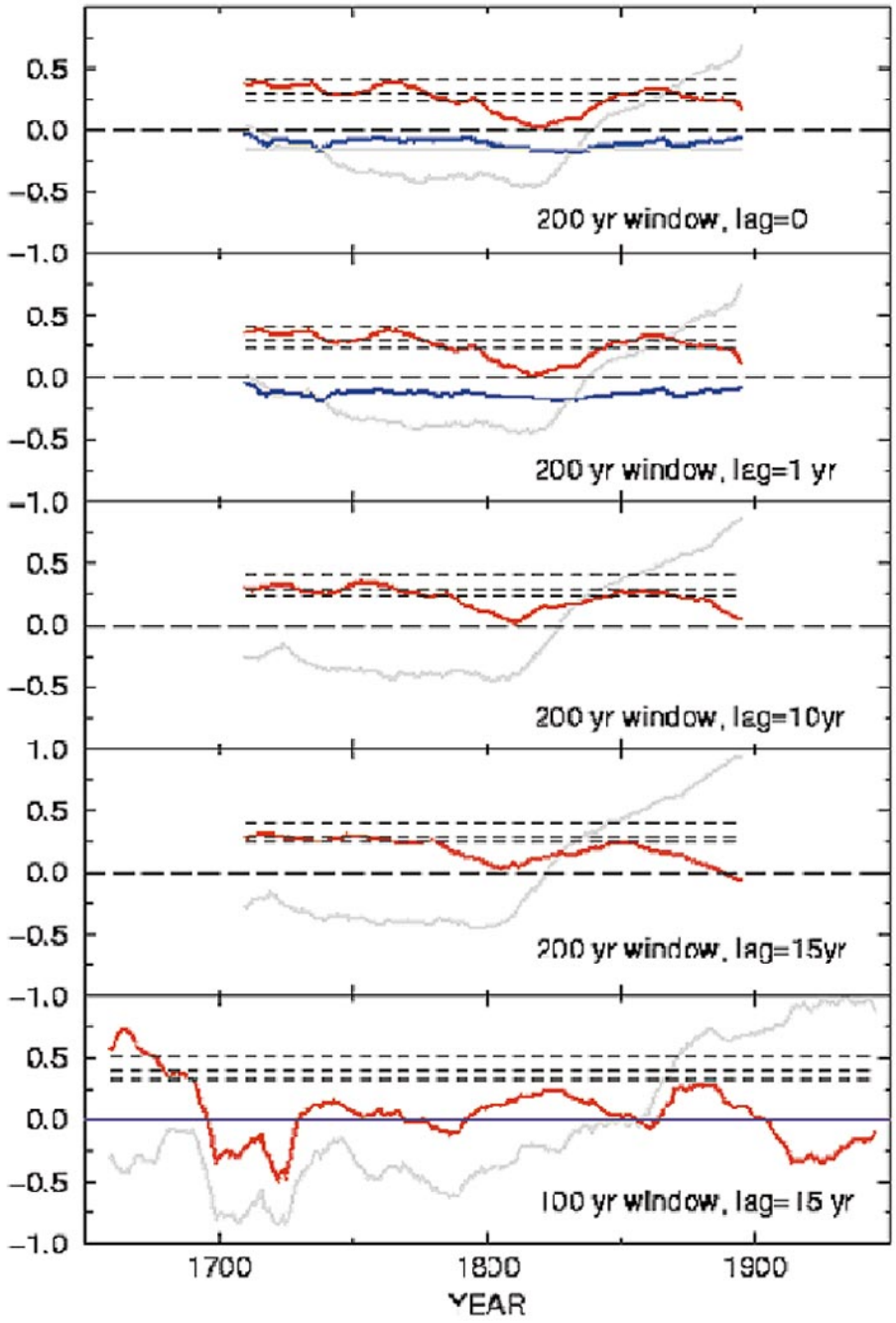

Figure 18. Relationship between NH series and forcings as above, but employing varying values of lag of temperatures relative to forcing. Symbols are same as above. The first five panels make use of the 200-yr window used

tical relationships with particular forcings. At the physically expected lag of 1 yr, the relationship between temperature variations and volcanic forcing is *slightly* more consistent and significant (at or near 95% significant for much of the interval examined, in contrast with the zero-lag case). For lags of 10–15 yr the relationship between greenhouse gas (GHG) increases in recent decades and increasing temperatures is considerably more significant, while the relationship with solar irradiance is considerably less significant. For the shorter (100 yr) window there are few enough degrees of freedom in the temperature and forcing series that the statistics are not as stable (i.e., the results are much ''noisier''). In particular, larger negative correlations with GHGs are achieved prior to 1800 in this case, although these are not significant taking into account the decreased degrees of freedom in the series. Nonetheless, even with the large sampling variations that arise in the 100-yr window case, the relationship between recent warming and increasing greenhouse gas concentrations is the dominant statistical feature. It is evident that the inclusion of a representation of the lagged response of temperatures to forcing heightens the evidence for a recent anthropogenic impact on twentieth century climate beyond that presented in Mann et al. (Mann et al., 1998).

4. Summary

A number of important conclusions are evident from the global-scale temperature reconstructions presented here. The sequences of annual and seasonal spatial temperature patterns presented in this study provide considerably more insight into the large-scale trends discussed in earlier work. The combination of multiple factors including El Niño/La Niña influences; interannual, decadal, and multidecadal patterns of extratropical variability; and putative responses to external forcings (such as volcanic aerosol loading of the upper atmosphere) leads to rich year-to-year spatial and temporal behavior that is readily documented in the annual temperature patterns. Considerable physical and dynamical insight into empirical climate variability over several centuries is thus obtained from the details of the patterns of annual and seasonal surface temperature variation. Some important new insights into the largest-scale climate trends are also available. As documented previously, not only is the global-scale warmth of the most recent decade observed to be quite unusual in the context of at least the past six centuries

←

Figure 18. (continued) above. In the first panel, we repeat the zero-lag case shown above for comparison, while the second panel shows the results for 1-yr lag, the third panel the 10-yr lag, and the fourth panel the 15-yr lag. The fifth panel shows the results based on employing a 100-yr moving window in the time-dependent attribution analysis, and with a 15-yr lag in the relationship of temperature to forcings. For lags much larger than 1 yr, the relationship of temperatures to volcanic forcing is not physically meaningful and is quite small. Thus, the relationship to volcanic forcing is not shown in the third, fourth, and fifth panels.

(and evidently, at least the past millennium), but 1998—the warmest year in the instrumental record—is seen to be truly exceptional in a long-term context. There is, however, a distinct latitudinal, seasonal, and spatial dependence evident in surface temperature trends during the past few centuries. Certain recent El Niño events (i.e., 1997–98 and 1982–83) also appear to be somewhat anomalous in the context of the past few centuries, though the recent trends in ENSO indices are not nearly as dramatic as those in the recent hemispheric warmth. Indeed, revised statistical attribution analyses comparing the hemispheric temperature series to candidate external forcings show greater evidence for a likely anthropogenic influence than that presented previously, when the potential for a lagged response of the climate system to radiative forcing (owing to oceanic thermal inertia) is taken into account.

It is clear that the primary limitations of large-scale proxy-based reconstruction in past centuries, both temporally and spatially, reside in the increasingly sparse nature of available proxy networks available to provide reliable climate information back in time. Only through the arduous efforts of large numbers of paleoclimate researchers can such networks be extended in space and time to the point where significant improvements will be possible in proxy-based reconstruction of the global climate. Such improvements will lead to further advances in our empirical understanding of climate variations during the past millennium and will allow for more meaningful comparisons with the results obtained from model simulations of past climate variation and empirical climate variability.

Acknowledgments. We thank Robin Webb and the NOAA Paleoclimatology Program for helping motivate this interactive project. We are also grateful to Martin Munro, Richard Holmes, and Caspar Ammann for their technical assistance. This work was supported by the National Science Foundation and NOAA-supported Earth Systems History Program, and the U.S. Department of Energy.

MEM acknowledges partial support through the Alexander Hollaender Distinguished Postdoctoral Research Fellowship Program of the U.S. Department of Energy. This work is a contribution to the NSF- and NOAA-sponsored Analysis of Rapid and Recent Climatic Change Project.

References

Barnett, T. P., B. Santer, P. D. Jones, and R. S. Bradley, 1996: Estimates of low frequency natural variability in near-surface air temperature. *Holocene*, **6**, 255–263.

Bradley, R. S., and P. D. Jones, 1993: 'Little Ice Age' summer temperature variations: Their nature and relevance to recent global warming trends. *Holocene*, **3**, 367–376.

Briffa, K. R., P. D. Jones, F. H. Schweingruber, and T. J. Osborn, 1998: Influence of volcanic eruptions on Northern Hemisphere summer temperature over the past 600 years. *Nature*, **393**, 350–354.

Crowley, T. J., and K.-Y. Kim, 1999: Modeling the temperature response to forced climate change over the last six centuries. *Geophys. Res. Lett.*, **26**, 1901–1904.

Crowley, T. J., and T. Lowery, 2000: How warm was the Medieval Warm Period? A comment on ''Man-made versus Natural Climate Change.'' *Ambio*, **29**, 51–54.

Cullen, H., R. D'Arrigo, E. Cook, and M. E. Mann, 2000: Multiproxy-based reconstructions of the North Atlantic oscillation over the past three centuries. *Paleoceanography*, in press.

Delworth, T. D., and M. E. Mann, 2000: Observed and simulated multidecadal variability in the Northern Hemisphere. *Clim. Dyn.*, **16**, 661–676.

Grove, J. M., and R. Switsur, 1994: Glacial geological evidence for the Medieval Warm Period. *Clim. Change,* **26**, 143–169.

Houghton, J. T., L. G. Meira Filho, B. A. Callander, N. Harris, A. Kattenberg, and K. Maskell, Eds., 1995*: Climate Change 1995: The Science of Climate Change.* Cambridge Univ. Press, 339 pp.

Hughes, M. K., and H. F. Diaz, 1994: Was there a 'Medieval Warm Period' and if so, where and when?. *Clim. Change,* **26**, 109–142.

Jones, P. D., 1994: Hemispheric surface air temperature variations: A reanalysis and an update to 1993. *J. Clim.*, **7**, 1794–1802.

Jones, P. D., K. R. Briffa, T. P. Barnett, and S. F. B. Tett, 1998: High-resolution paleoclimatic records for the last millennium: Interpretation, integration and comparison with circulation model control run temperatures. *Holocene,* **8**, 455–471.

Jones, P. D., M. New, D. E. Parker, S. Martin, and I. G. Rigor, 1999: Surface air temperature and its changes over the past 150 years. *Rev. Geophys.,* **37**, 173–199.

Lean, J., J. Beer, and R. S. Bradley, 1995: Reconstruction of solar irradiance since 1610: Implications for climatic change. *Geophys. Res. Lett.,* **22**, 3195–3198.

Luterbacher, J., C. Schmutz, D. Gyalistras, E. Xoplaki, and H. Wanner, 1999: Reconstruction of monthly NAO and EU indices back to AD 1675. *Geophys. Res. Lett.*, **26**, 2745–2749.

Mann, M. E., 2000: Large-scale climate variability and connections with the Middle East in past centuries. *Clim. Change,* in press.

Mann, M. E., J. Park, and R. S. Bradley, 1995: Global interdecadal and century-scale climate oscillations during the past five centuries,. *Nature,* **378**, 266–270.

Mann, M. E., R. S. Bradley, and M. K. Hughes, 1998: Global-scale temperature patterns and climate forcing over the past six centuries. *Nature,* **392**, 779–787.

Mann, M. E., R. S. Bradley, and M. K. Hughes, 1999: Northern Hemisphere temperatures during the past millennium: Inferences, uncertainties, and limitations. *Geophys. Res. Lett.,* **26**, 759–762.

Mann, M. E., R. S. Bradley, and M. K. Hughes, 2000: Long-term variability in the El Niño Southern Oscillation and associated teleconnections. *El Niño and the Southern Oscillation: Multiscale Variability and Its Impacts on Natural Ecosystems and Society*, edited by H. F. Diaz and V. Markgraf, Cambridge Univ. Press, 357–412.

Ortlieb, L., 2000: The documentary historical record of El Niño events in Peru: An update of the Quinn record (sixteenth through nineteenth centuries). *El Niño and the Southern Oscillation: Multiscale Variability and its Impacts on Natural Ecosystems and Society*, edited by H. F. Diaz and V. Markgraf, Cambridge Univ. Press, 207–295.

Overpeck, J., 1998: How unprecedented is recent Arctic warming: A look back to the Medieval Warm Period (abstract). *Eos, Trans AGU,* **79** (Suppl.), 833–834.

Overpeck, J., K. Hughen, D. Hardy, R. Bradley, R. Case, M. Douglas, B. Finney, K. Gajewski, G. Jacoby, A. Jennings, S. Lamoureux, A. Lasca, G. Macdonald, J. Moore, M. Retelle, S. Smith, A. Wolfe, and G. Zielinski, 1997: Arctic environmental changes of the last four centuries. *Science,* **278**, 1251–1256.

Pollack, H., S. Huang, and P. Y. Shen, 1998: Climate change revealed by subsurface temperatures: A global perspective. *Science,* **282**, 279–281.

Quinn, W. H., and V. T. Neal, 1992: The historical record of El Niño events. *Climate Since A.D. 1500,* edited by R. S. Bradley and P. D. Jones, Routledge, New York, 623–648.

Robertson, A. D., J. T. Overpeck, E. Mosley-Thompson, G. A. Zielinski, J. L. Lean, D. Koch, J. E. Penner, I. Tegen, D. Rind, and R. Healy, 1998: Hypothesized climate forcing time series for the last 500 years (abstract). *Eos, Trans. AGU,* **79** (Suppl.), 833–834.

Stahle, D.W., M. K. Cleaveland, M. D. Therrell, D. A. Gay, R. D. D'Arrigo, P. J. Krusic, E. R. Cook, R. J. Allan, J. E. Cole, R. B. Dunbar, M. D. Moore, M. A. Stokes, B. T. Burns, J.

Villanueva-Diaz, and L. G. Thompson, 1998: Experimental dendroclimatic reconstruction of the Southern Oscillation. *Bull. Am. Meteorol. Soc.*, **79**, 2137–2152.

Waple, A., M. E. Mann, and R. S. Bradley, 2000: Long-term patterns of solar irradiance forcing in model experiments and proxy-based surface temperature reconstructions. *Clim. Dyn.*, in press.